



Supplementary Information for

THE FEEDING SYSTEM OF *TIKTAALIK ROSEAE*: AN INTERMEDIATE BETWEEN SUCTION  
FEEDING AND BITING

Justin B. Lemberg, Edward B. Daeschler, Neil H. Shubin

Corresponding authors: Justin B. Lemberg, Neil H. Shubin

Email: Justin B. Lemberg, [lemberg@uchicago.edu](mailto:lemberg@uchicago.edu); Neil H. Shubin, [nshubin@uchicago.edu](mailto:nshubin@uchicago.edu)

**This PDF file includes:**

Figures S1 to S8

Tables S1 to S3

Legends for Movies S1 to S2

**Other supplementary materials for this manuscript include the following:**

Movies S1 to S2

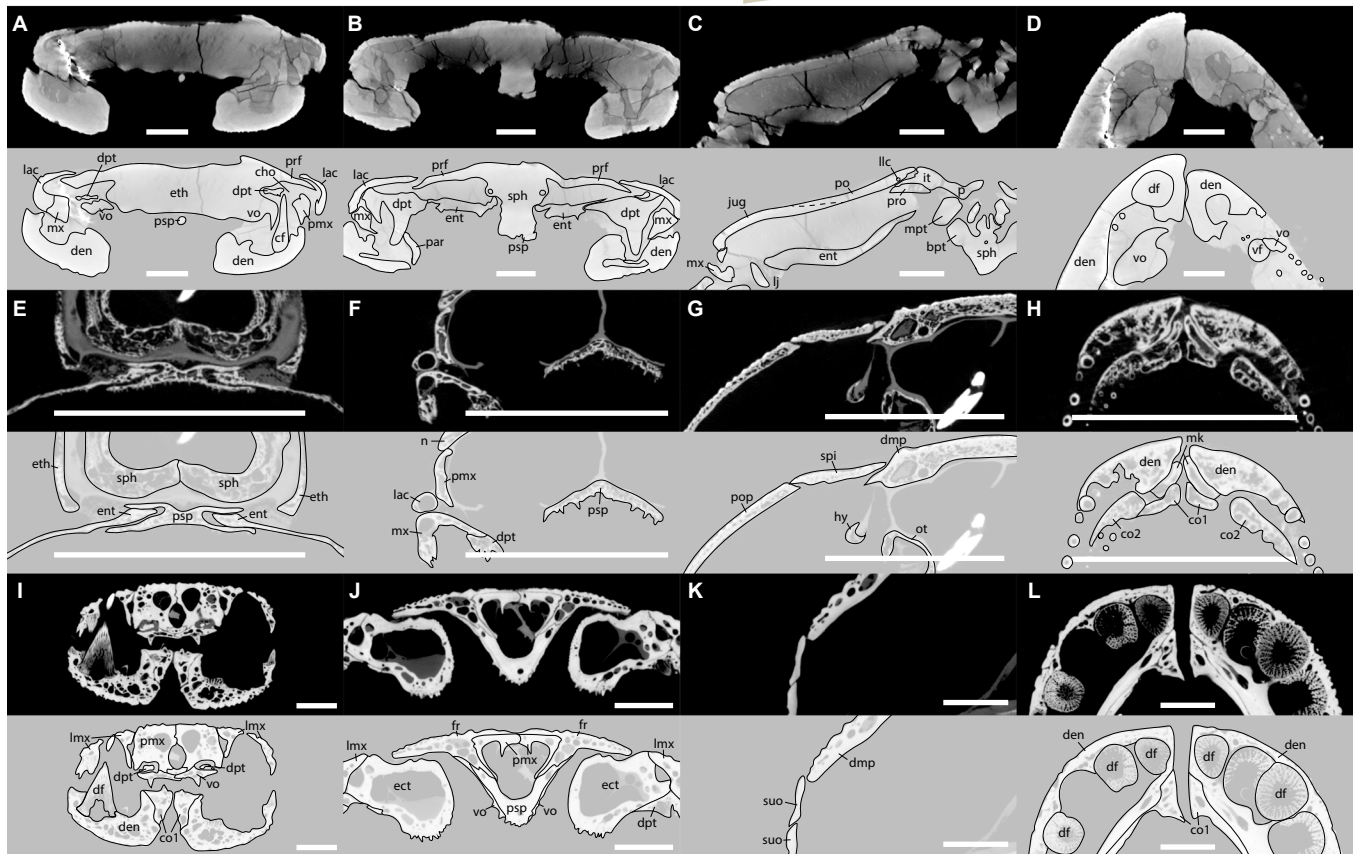
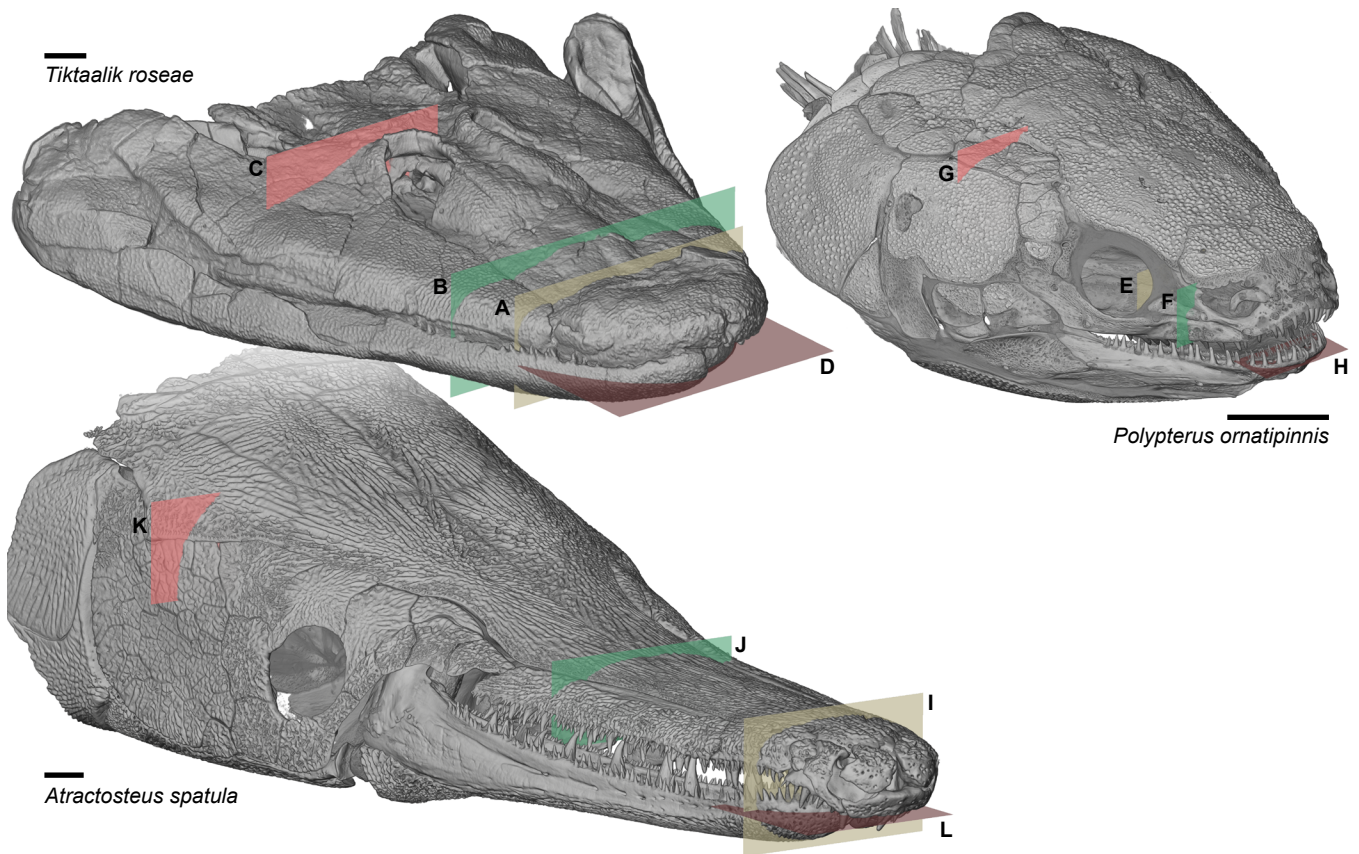


**Figure S1 | Comparison of analogous joints in *Tiktaalik roseae*, *Polypterus ornatipinnis*, *Atractosteus spatula*.** (Top) 3D cranial volume renderings showing positioning of slice cross sections (below) for  $\mu$ CT scans of (A-D) *T. roseae* (NUFV 108), (E-H) *P. ornatipinnis* (FMNH 121744), and (I-L) *A. spatula* (FMNH 119220D). (A,E,I) Primary anterior attachment of the palate to the braincase. (B,F,J) Preorbital cross section of the interface between the cheek and dermal bones of the rostrum. (C,G,K) Postorbital cross section of the interface between the cheek and dermal bones of the skull table. (D,H,L) Cross section of the mandibular symphysis. Abbreviations: bpt, basipterygoid process; cf, coronoid fang; cho, choana; co1, first coronoid; co2, second coronoid; den, dentary; df, dentary fang; dmp, dermopterotic; dpt, dermopalatine; ect, ectopterygoid; ent, endopterygoid; eth, ethmoid region of braincase; fr, frontal; hy, hyomandibula; it, intertemporal; jug, jugal; lac, lacrimal; lj, lower jaw; llc, lateral line canal; lmx, lacrimomaxilla; mk, mentomeckelian; mpt, metapterygoid; mx, maxilla; n, nasal; ot, otic region of braincase; p, parietal; par, prearticular; pmx, premaxilla; po, postorbital; pop, preopercle; prf, prefrontal; pro, prootic process; psp, parasphenoid; sph, sphenoid region of braincase; spi, spiracular bones; suo, suborbital; vf, vomerine fang; vo, vomer. Scale bars = 1cm.

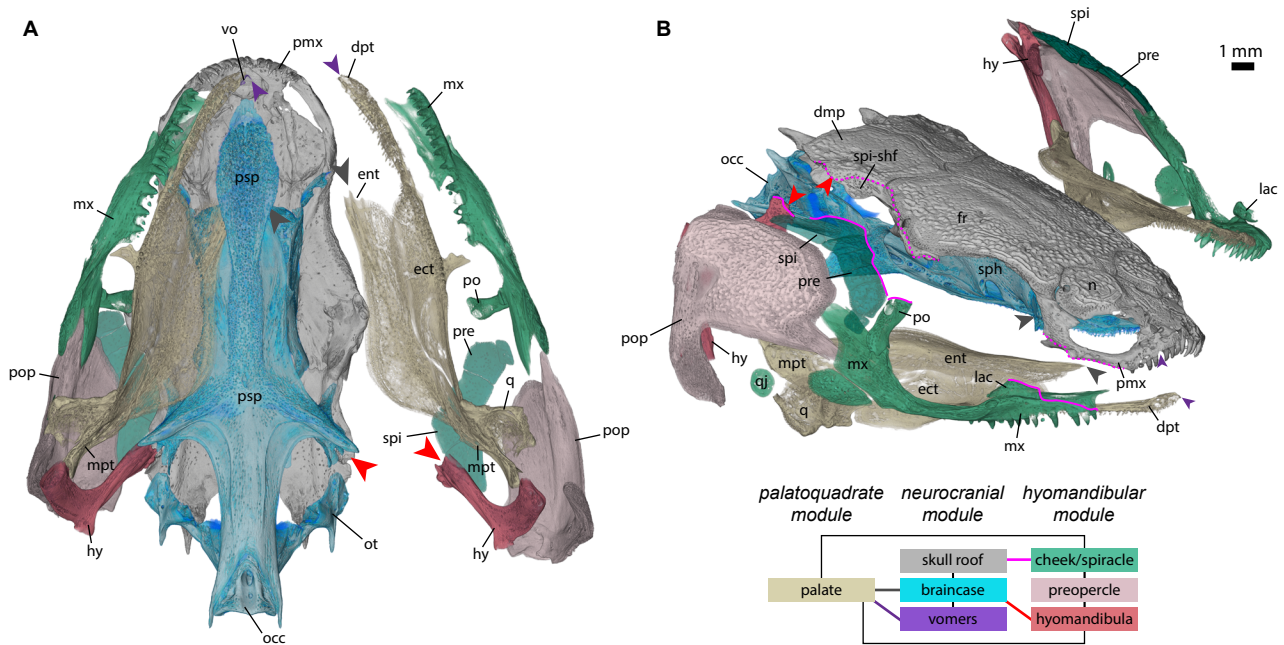


**Figure S2 | Functional modularity of the skull of *Polypterus ornatipinnis*.** Disarticulated skull of *P. ornatipinnis* (FMNH 117746) in (A) ventral and (B) antero-dorsolateral right oblique views. Bones of distinct regions are color coded by anatomical unit: cheek (green), palate (yellow), skull roof (grey), braincase (cyan), vomers (purple), hyomandibula (red). These anatomical units are further grouped by functional modules, which have clear mobile articulations with other modules but otherwise appear to be functionally integrated and immobile within themselves. Articulations of the ‘palatoquadrate module’ (palate) with the ‘neurocranial module’ (dermal skull roof, braincase, vomers) include the endopterygoid-parasphenoid (grey arrow, Fig. S1e), and dermopalatine-vomerine (purple arrow). Articulations of the ‘hyomandibular module’ (hyomandibula, cheek, spiracular series, and preopercle) with the ‘neurocranial module’ include the lacrimal-premaxilla (magenta line, Fig. S1f), ‘spiracular-shelf’ (spi-shf, magenta line, Fig. S1g), and the hyomandibular-dermopterotic (red arrow). Articulations of the ‘palatoquadrate module’ with the ‘hyomandibular module’ include the dermopalatine-maxilla (Fig. S1f). Abbreviations: dmp, dermopterotic; dpt, dermopalatine; ect, ectopterygoid; ent, endopterygoid; fr, frontal; hy, hyomandibula; lac, lacrimal; mpt, metapterygoid; mx, maxilla; n, nasal; occ, occipital region of braincase; ot, otic region of braincase; pmx, premaxilla; po, postinfraorbital; pop, preopercle; pre, prespiracular bone series; psp, parasphenoid; q, quadrate; qj, quadratojugal; sph, sphenoid region of braincase; spi, spiracular plates; spi-shf, ‘spiracular shelf’ of the dermopterotic; vo, vomer.



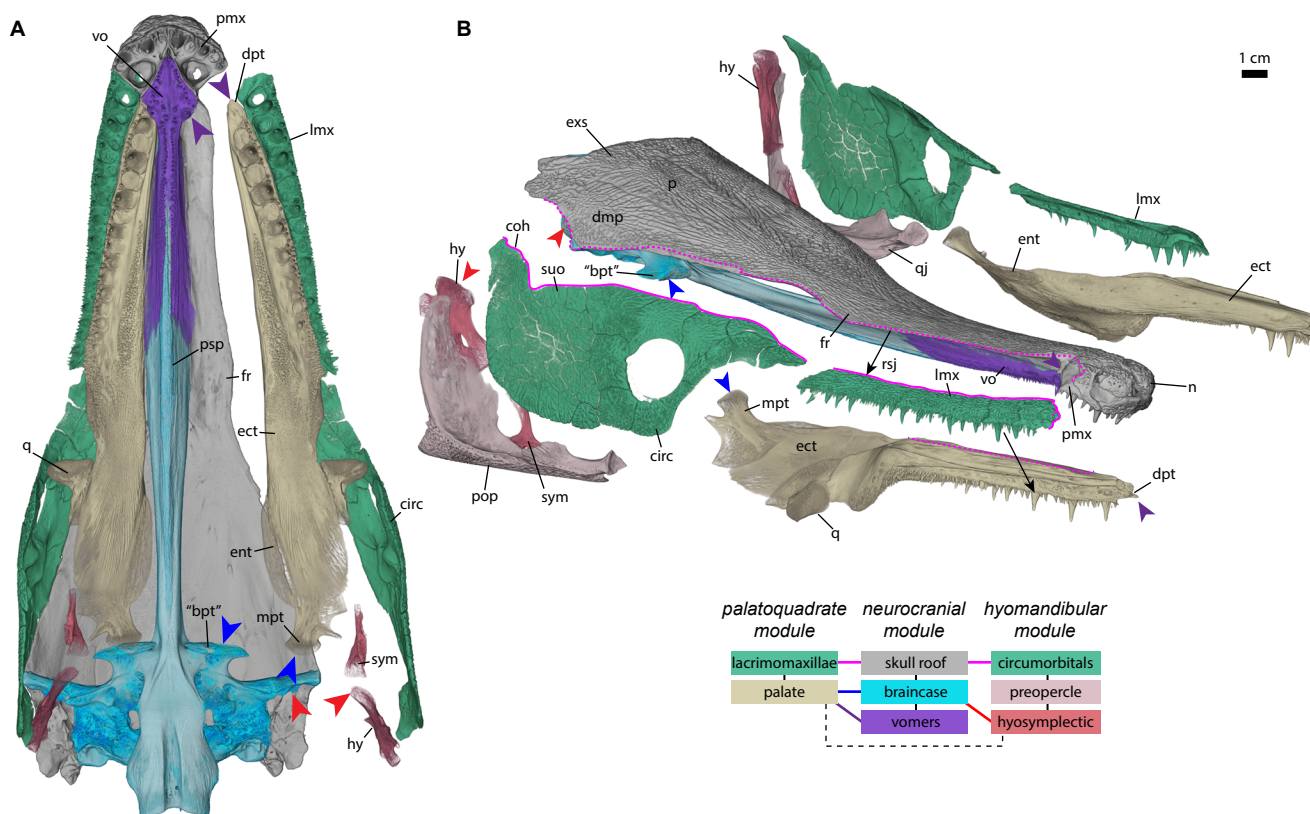


**Figure S3 | Functional modularity of the skull of *Atractosteus spatula*.** Disarticulated skull of *A. spatula* (FMNH 119220D) in (A) ventral and (B) antero-dorsolateral right oblique views. Bones of distinct regions are color coded by anatomical unit: cheek (green), palate (yellow), skull roof (grey), braincase (cyan), vomers (purple), hyomandibula (red). These anatomical units are further grouped by functional modules, which have clear mobile articulations with other modules but otherwise appear to be functionally integrated and immobile within themselves. Articulations of the ‘palatoquadrate module’ (palate, lacrimomaxillae) with the ‘neurocranial module’ (dermal skull roof, braincase, vomers) include the metapterygoid-basipterygoid process (blue arrow), dermopalatine-vomerine (purple arrow, Fig. S1i), and ‘rostral scarf joint’ (rsj, magenta line, Fig. S1j). Articulations of the ‘hyomandibular module’ (hyosymplectic, circumorbitals/suborbitals, and preopercle) with the ‘neurocranial module’ include the hyomandibular-dermopterotic (red arrow) and the ‘circumorbital hinge’ (coh, magenta line, Fig. S1k). Articulation of the ‘palatoquadrate module’ with the ‘hyomandibular module’ is entirely cartilaginous. Abbreviations: “bpt”, basipterygoid process (non-homologous to tetrapods); circ, circumorbitals; coh, circumorbital hinge; dmp, dermopterotic; dpt, dermopalatine; ect, ectopterygoid; ent, endopterygoid; exs, extrascapulars; fr, frontal; hy, hyomandibula; lmx, lacrimomaxilla; mpt, metapterygoid; n, nasal; p, parietal; pmx, premaxilla; pop, preopercle; psp, parasphenoid; q, quadrate; qj, quadratojugal; rsj, rostral scarf joint; suo, suborbital; sym, symplectic; vo, vomer.

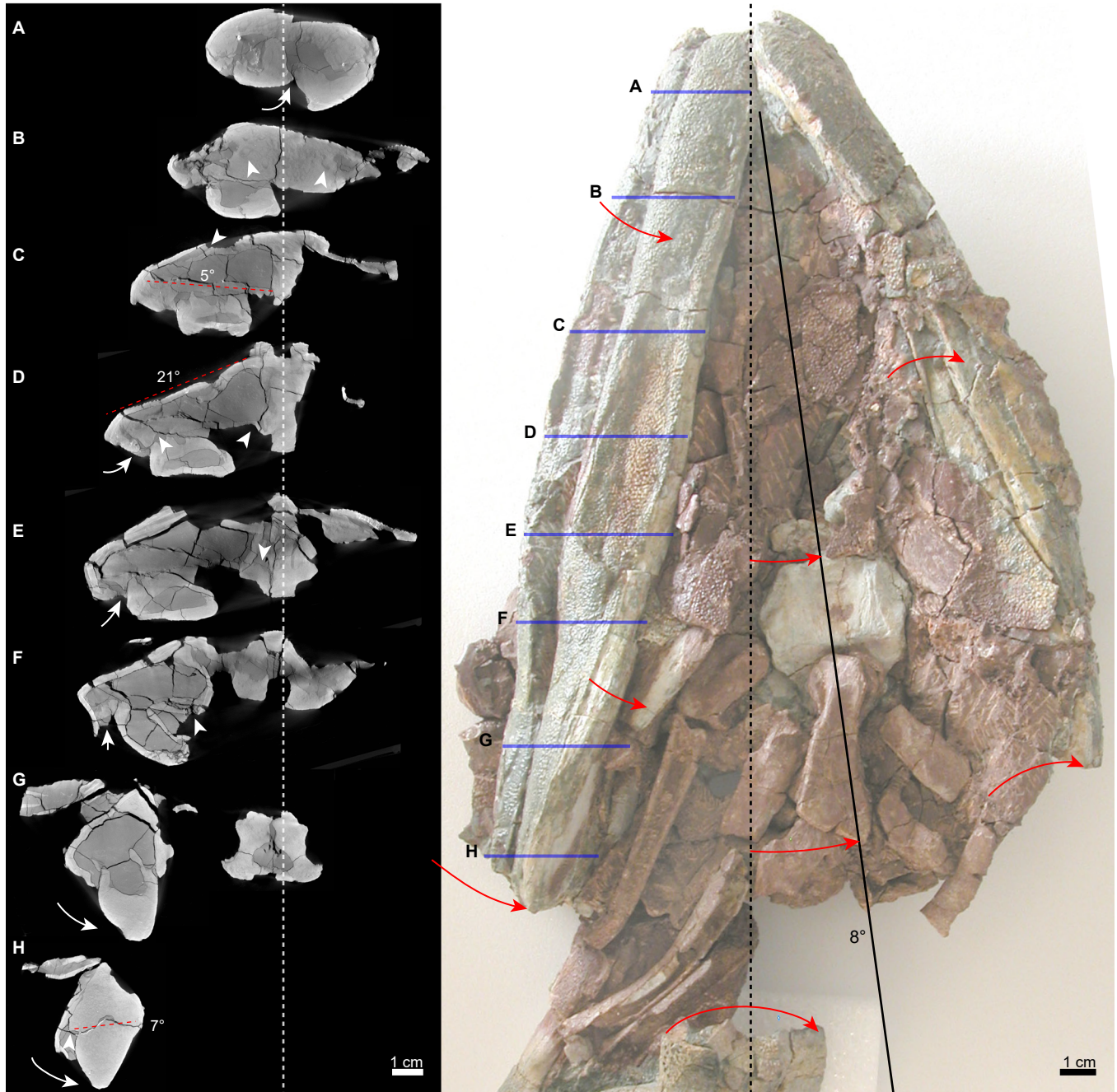


**Figure S4 | Postmortem deformation patterns of *Tiktaalik roseae* (NUFV 110).** (Left, a-h) cross sections that show significant areas of postmortem breakage and displacement (white arrows) relative to the midline of the braincase (dashed-line). (Right) articulated ventral view of cranial elements and pectoral fin elements showing orientation of the midline of the braincase (dashed-line) and hypothesized displacement (red arrows) of cranial elements towards a visible midline of ventral elements (solid line) on the left-hand side of the specimen. Deformation patterns are consistent with a skull that has been laterally compressed on the right lateral side during the preservation process, which has uniformly displaced ventral elements towards the left side of the specimen.



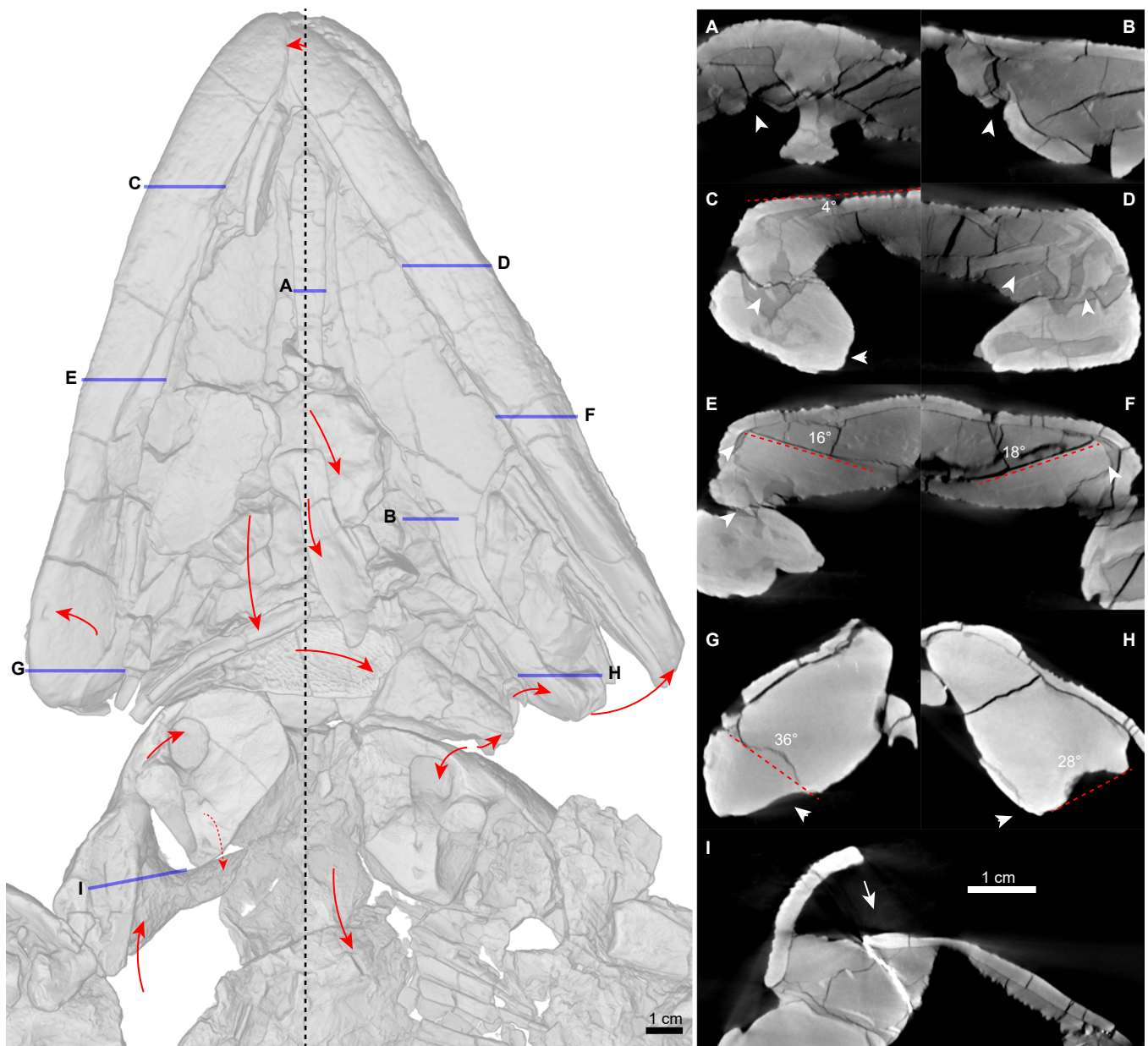


**Figure S5 | Postmortem deformation patterns of the holotype specimen of *Tiktaalik roseae* (NUFV 108).** (Left) articulated ventral view of cranial elements and pectoral fin elements showing orientation of the midline of the braincase (dashed-line) and hypothesized displacement (red arrows) of cranial elements off that midline. (Right) corresponding cross sections that show significant areas of postmortem breakage (white arrows). Deformation patterns are consistent with a skull that has been partially dorsoventrally compressed during the preservation process.

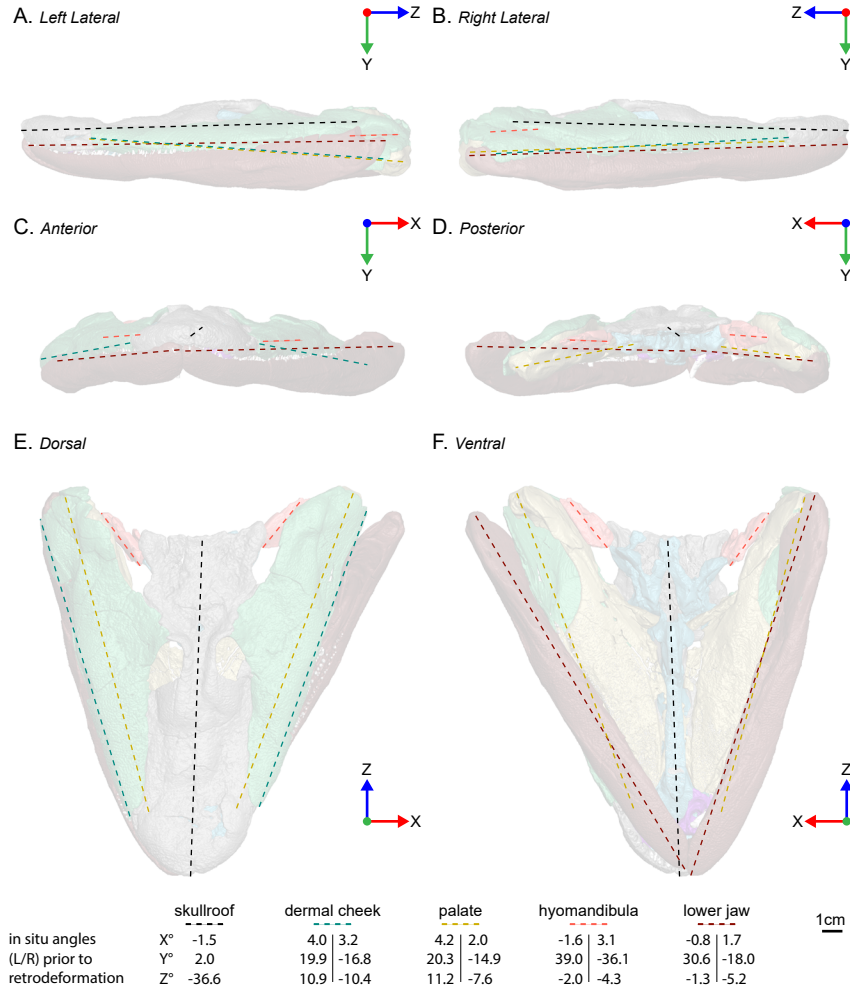


**Figure S6 | *In situ* positions of cranial elements of *Tiktaalik roseae* (NUFV 108) prior to retrodeformation.** (Top) Shown are the six orthogonal views (X = right/left; Y = dorsal/ventral; Z = anterior/posterior) of the skull of NUFV 108, with highlighted positional vectors (dashed lines) showing the relative angles (below) of these elements in X/Y/Z. Vectors include: the skull roof from the tip of the rostrum to the back of the skull table (black); the dermal cheek from the lacrimal-anterior-tectal joint to posterolateral-most point of the quadratojugal (green); the palate from the dermopalatine-vomerine joint to the jaw-joint (yellow); the hyomandibula from its articulation with the lateral-commissure to the most distal, ossified portion (salmon); the jaw from the mandibular symphysis to the retroarticular process (dark red).



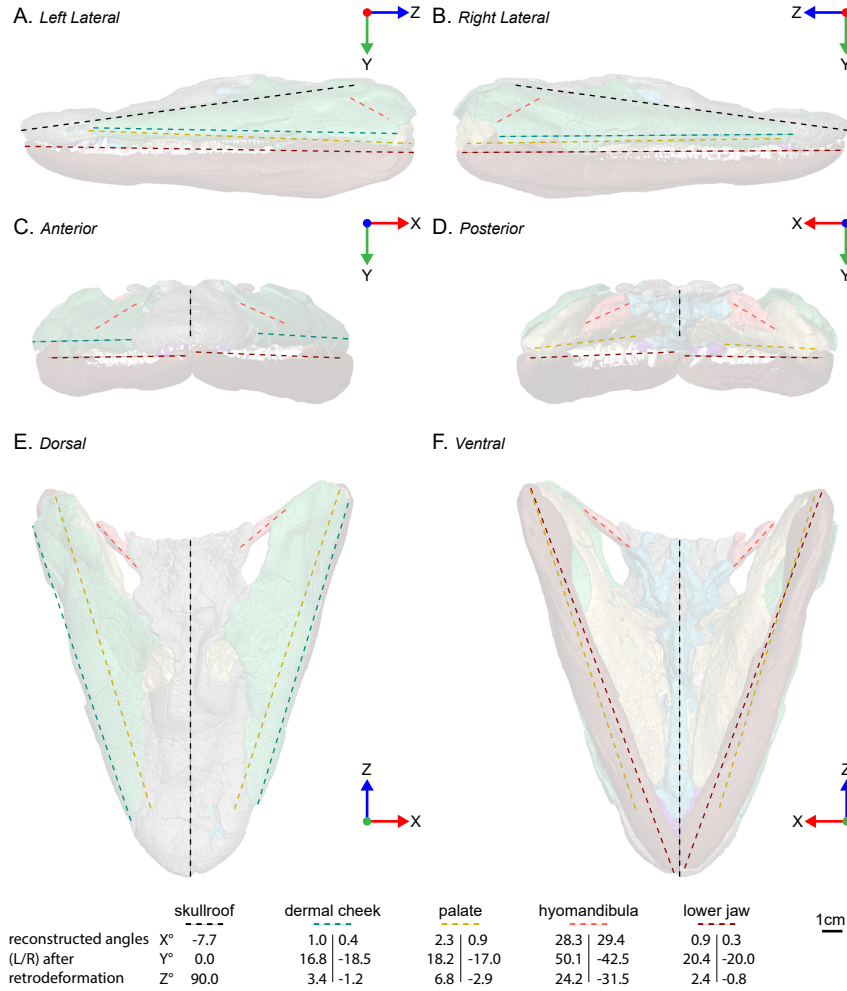


**Figure S7 | Estimated *in vivo* positions of cranial elements of *Tiktaalik roseae* (NUFV 108) after retrodeformation.** (Top) Shown are the six orthogonal views (X = right/left; Y = dorsal/ventral; Z = anterior/posterior) of the skull of NUFV 108, with highlighted positional vectors (dashed lines) showing the relative angles (below) of these elements after retrodeformation in X/Y/Z. Vectors include: the skull roof from the tip of the rostrum to the back of the skull table (black); the dermal cheek from the lacrimal-anterior-tectal joint to posterolateral-most point of the quadratojugal (green); the palate from the dermopalatine-vomerine joint to the jaw-joint (yellow); the hyomandibula from its articulation with the lateral-commissure to the most distal, ossified portion (salmon); the jaw from the mandibular symphysis to the retroarticular process (dark red).

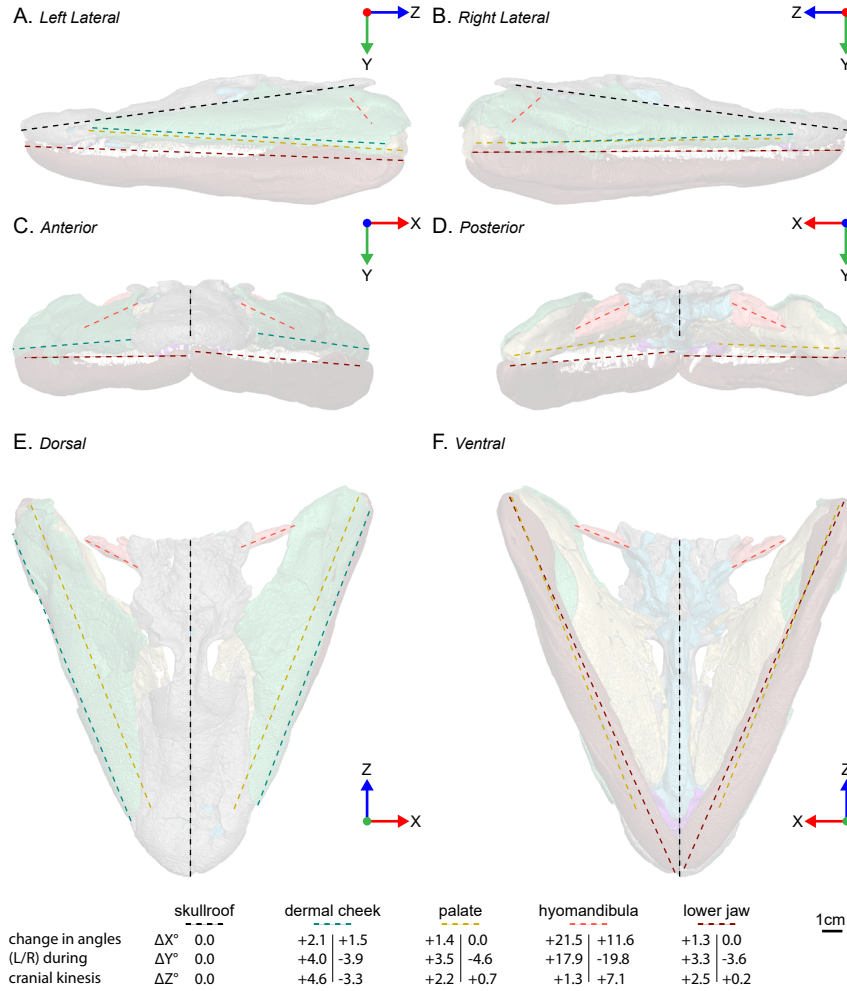


**Figure S8 | Modeled expanded-state positions of cranial elements of *Tiktaalik roseae* (NUFV 108) due to cranial kinesis.** (Top) Shown are the six orthogonal views (X = right/left; Y = dorsal/ventral; Z = anterior/posterior) of the skull of NUFV 108, with highlighted positional vectors (dashed lines) showing change in angles (below) of these elements due to cranial kinesis in X/Y/Z. Vectors include: the skull roof from the tip of the rostrum to the back of the skull table (black); the dermal cheek from the lacrimal-anterior-tectal joint to posterolateral-most point of the quadratojugal (green); the palate from the dermopalatine-vomerine joint to the jaw-joint (yellow); the hyomandibula from its articulation with the lateral-commissure to the most distal, ossified portion (salmon); the jaw from the mandibular symphysis to the retroarticular process (dark red).

**Table S1 |  $\mu$ CT scanning parameters of referenced specimens. Each row represents an individually scanned cranial element with voltage, current, filter, and resolution provided.** All scans were collected using a GE Phoenix v|tome|x 240 kv/180kv scanner and are deposited on MorphoSource (P1213, [https://www.morphosource.org/Detail/ProjectDetail/Show/project\\_id/1213](https://www.morphosource.org/Detail/ProjectDetail/Show/project_id/1213)).

specimen	element	tube	voltage	current	filter	voxel size	DOI
<i>Tiktaalik roseae</i>							
NUFV 108	skull (complete)	240	100 kV	590 $\mu$ A	0.24 mm Cu	109.8660 $\mu$ m	<a href="https://doi.org/10.17602/M2/M168208">https://doi.org/10.17602/M2/M168208</a>
NUFV 108	skull table (high-res)	240	100 kV	580 $\mu$ A	0.24 mm Cu	66.4100 $\mu$ m	<a href="https://doi.org/10.17602/M2/M168245">https://doi.org/10.17602/M2/M168245</a>
NUFV 109	snout	240	130 kV	500 $\mu$ A	0.48 mm Sn 0.50 mm Cu	68.2370 $\mu$ m	<a href="https://doi.org/10.17602/M2/M168246">https://doi.org/10.17602/M2/M168246</a>
NUFV 109	palate (right)	240	130 kV	500 $\mu$ A	0.48 mm Sn 0.50 mm Cu	68.2370 $\mu$ m	<a href="https://doi.org/10.17602/M2/M168247">https://doi.org/10.17602/M2/M168247</a>
NUFV 109	palate (left, anterior)	240	130 kV	500 $\mu$ A	0.48 mm Sn 0.50 mm Cu	68.2370 $\mu$ m	<a href="https://doi.org/10.17602/M2/M168248">https://doi.org/10.17602/M2/M168248</a>
NUFV 109	palate (left, posterior)	240	130 kV	500 $\mu$ A	0.48 mm Sn 0.50 mm Cu	68.2370 $\mu$ m	<a href="https://doi.org/10.17602/M2/M168249">https://doi.org/10.17602/M2/M168249</a>
NUFV 109	temporal roofing bones (right)	240	130 kV	500 $\mu$ A	0.48 mm Sn 0.50 mm Cu	68.2370 $\mu$ m	<a href="https://doi.org/10.17602/M2/M168363">https://doi.org/10.17602/M2/M168363</a>
NUFV 109	basisphenoid	240	130 kV	500 $\mu$ A	0.48 mm Sn 0.50 mm Cu	68.2370 $\mu$ m	<a href="https://doi.org/10.17602/M2/M169918">https://doi.org/10.17602/M2/M169918</a>
NUFV 110	palate (left)	180	110 kV	95 $\mu$ A	none	37.1720 $\mu$ m	<a href="https://doi.org/10.17602/M2/M169417">https://doi.org/10.17602/M2/M169417</a>
NUFV 110	skull (braincase, right cheek, and palate)	240	90 kV	390 $\mu$ A	0.24 mm Cu	59.3900 $\mu$ m	<a href="https://doi.org/10.17602/M2/M169232">https://doi.org/10.17602/M2/M169232</a>
NUFV 111	snout	180	105 kV	100 $\mu$ A	none	34.4720 $\mu$ m	<a href="https://doi.org/10.17602/M2/M168952">https://doi.org/10.17602/M2/M168952</a>
NUFV 119	snout	240	80 kV	380 $\mu$ A	none	32.3390 $\mu$ m	<a href="https://doi.org/10.17602/M2/M168757">https://doi.org/10.17602/M2/M168757</a>
NUFV 149	braincase and palate	180	90 kV	115 $\mu$ A	none	24.3080 $\mu$ m	<a href="https://doi.org/10.17602/M2/M168955">https://doi.org/10.17602/M2/M168955</a>
NUFV 149	rostral portions of upper and lower jaws	240	110 kV	170 $\mu$ A	0.12 mm Cu	52.8280 $\mu$ m	<a href="https://doi.org/10.17602/M2/M168954">https://doi.org/10.17602/M2/M168954</a>
<i>Atractosteus spatula</i>							
FMNH 119220D	skull (complete)	240	190 kV	280 $\mu$ A	none	106.436 $\mu$ m	<a href="https://doi.org/10.17602/M2/M168210">https://doi.org/10.17602/M2/M168210</a>
<i>Polypterus ornatipinnis</i>							
FMNH 117746	skull (complete)	240	150 kV	100 $\mu$ A	none	15.8540 $\mu$ m	<a href="https://doi.org/10.17602/M2/M168211">https://doi.org/10.17602/M2/M168211</a>
FMNH 121744	skull (complete)	240	190 kV	180 $\mu$ A	none	35.0190 $\mu$ m	<a href="https://doi.org/10.17602/M2/M168212">https://doi.org/10.17602/M2/M168212</a>

**Table S2 | Retrodeformation parameters.** Transformation matrices in column vector notation used to reposition cranial elements of NUFV 108 during limited retrodeformation (translation and rotation only, no scaling or plastic deformation). Each matrix is decomposed into the equivalent changes in angle and position of the given cranial element.

*Midline bones (dermatocranium and chondrocranium):*

$$\begin{bmatrix} 0.997827 & 0.056818 & -0.033343 & 8.106230 \\ -0.060081 & 0.992463 & -0.106793 & -25.642600 \\ 0.027024 & 0.108566 & 0.993720 & -5.026390 \\ 0 & 0 & 0 & 1 \end{bmatrix} \equiv \begin{matrix} x' = 6.2^\circ & 6.046 \text{ mm} \\ y' = 2.0^\circ & -40.575 \text{ mm} \\ z' = 53.4^\circ & -1.110 \text{ mm} \end{matrix}$$

*Left cheek:*

$$\begin{bmatrix} 0.993175 & -0.107394 & -0.045494 & 13.096500 \\ 0.103087 & 0.990743 & -0.088296 & -43.781200 \\ 0.054556 & 0.083005 & 0.995053 & -7.392440 \\ 0 & 0 & 0 & 1 \end{bmatrix} \equiv \begin{matrix} x' = 3.0^\circ & 4.455 \text{ mm} \\ y' = 3.2^\circ & -40.984 \text{ mm} \\ z' = 7.5^\circ & 0.970 \text{ mm} \end{matrix}$$

*Right cheek:*

$$\begin{bmatrix} 0.990909 & 0.128601 & -0.039404 & 8.295270 \\ -0.131611 & 0.987484 & -0.086865 & -22.966700 \\ 0.027740 & 0.091263 & 0.995436 & -6.216320 \\ 0 & 0 & 0 & 1 \end{bmatrix} \equiv \begin{matrix} x' = 2.7^\circ & 6.292 \text{ mm} \\ y' = 1.7^\circ & -37.723 \text{ mm} \\ z' = -9.1^\circ & -3.781 \text{ mm} \end{matrix}$$

*Left palate:*

$$\begin{bmatrix} 0.984212 & -0.176138 & -0.017383 & 14.213600 \\ 0.173717 & 0.980132 & -0.095740 & -48.090100 \\ 0.033901 & 0.091210 & 0.995254 & -6.397620 \\ 0 & 0 & 0 & 1 \end{bmatrix} \equiv \begin{matrix} x' = 1.9^\circ & 5.645 \text{ mm} \\ y' = 2.1^\circ & -38.778 \text{ mm} \\ z' = 4.3^\circ & -0.454 \text{ mm} \end{matrix}$$

*Right palate:*

$$\begin{bmatrix} 0.976173 & 0.210866 & -0.051160 & 7.844360 \\ -0.214342 & 0.973782 & -0.076156 & -16.591300 \\ 0.033760 & 0.085309 & 0.995778 & -2.624910 \\ 0 & 0 & 0 & 1 \end{bmatrix} \equiv \begin{matrix} x' = 1.1^\circ & 5.742 \text{ mm} \\ y' = 2.1^\circ & -35.081 \text{ mm} \\ z' = -4.7^\circ & 0.269 \text{ mm} \end{matrix}$$

*Left hyomandibula:*

$$\begin{bmatrix} 0.548837 & -0.692434 & 0.467925 & -14.174400 \\ 0.828935 & 0.497982 & -0.238426 & -92.302600 \\ -0.067572 & 0.518075 & 0.847843 & 21.039400 \\ 0 & 0 & 0 & 1 \end{bmatrix} \equiv \begin{matrix} x' = -29.9^\circ & -1.169 \text{ mm} \\ y' = -11.1^\circ & -43.821 \text{ mm} \\ z' = -26.2^\circ & -3.178 \text{ mm} \end{matrix}$$



*Right hyomandibula:*

$$\begin{bmatrix} 0.866777 & 0.470180 & -0.166203 & 31.582900 \\ -0.461548 & 0.882570 & 0.089687 & -33.945500 \\ 0.188854 & -0.001025 & 0.981999 & -8.422680 \\ 0 & 0 & 0 & 1 \end{bmatrix} \equiv \begin{matrix} x' = -26.2^\circ & 6.697 \text{ mm} \\ y' = 6.4^\circ & + -41.857 \text{ mm} \\ z' = 27.3^\circ & -2.986 \text{ mm} \end{matrix}$$

*Left lower jaw:*

$$\begin{bmatrix} 0.973006 & 0.157917 & -0.168270 & 13.377000 \\ -0.140127 & 0.983671 & 0.112889 & -20.404800 \\ 0.183349 & -0.086262 & 0.979250 & -13.865300 \\ 0 & 0 & 0 & 1 \end{bmatrix} \equiv \begin{matrix} x' = -1.6^\circ & -1.186 \text{ mm} \\ y' = 10.2^\circ & + -27.887 \text{ mm} \\ z' = -3.7^\circ & 4.692 \text{ mm} \end{matrix}$$

*Right lower jaw:*

$$\begin{bmatrix} 0.963654 & 0.261675 & -0.053800 & 7.985340 \\ -0.266176 & 0.957646 & -0.109823 & -7.171140 \\ 0.022785 & 0.120152 & 0.992494 & -1.972400 \\ 0 & 0 & 0 & 1 \end{bmatrix} \equiv \begin{matrix} x' = 1.4^\circ & 10.213 \text{ mm} \\ y' = 2.0^\circ & + -30.186 \text{ mm} \\ z' = -4.4^\circ & 2.337 \text{ mm} \end{matrix}$$

**Table S3 | Cranial kinesis parameters.** Rotation matrices and vectors used to define rotation of cranial elements of NUFV 108 during cranial kinesis. Matrices are presented in column vector notation, and vectors describe the position (X/Y/Z) in mm of a given anatomical landmark relative to the point of rotation within the same anatomical unit before and after rotation. Each vector also allows angles to be calculated ( $X^\circ/Y^\circ/Z^\circ$ ) by taking the inverse tangent of the other two values (e.g.  $X^\circ = \tan^{-1}(Y/Z)$ ) and the change of angles around each axis due to cranial kinesis are provided.

*Chondrocranium / Dermatocranium:*

Rotation of the back of the skull table relative to the tip of the rostrum:

$$\begin{bmatrix} 1 & 0 & 0 \\ 0 & 1 & 0 \\ 0 & 0 & 1 \end{bmatrix} \times \begin{bmatrix} 0.0 \\ -22.6 \\ 166.5 \end{bmatrix} = \begin{bmatrix} 0.0 \\ -22.6 \\ 166.5 \end{bmatrix} \equiv \begin{matrix} 0^\circ \text{ around } x \\ 0^\circ \text{ around } y \\ 0^\circ \text{ around } z \end{matrix}$$

*vector magnitude = 168.0 mm*

*External cheek:*

Rotation of the posterolateral-most point of the quadratojugal around the lacrimal-anterior tectal joint:

*Left:*

$$\begin{bmatrix} 0.9975 & -0.0082 & 0.0702 \\ 0.0059 & 0.9994 & 0.0327 \\ -0.0704 & -0.0322 & 0.9970 \end{bmatrix} \times \begin{bmatrix} 45.2 \\ 2.7 \\ 150.2 \end{bmatrix} = \begin{bmatrix} 55.6 \\ 7.9 \\ 146.5 \end{bmatrix} \equiv \begin{matrix} 2.1^\circ \text{ around } x \\ 4.0^\circ \text{ around } y \\ 4.6^\circ \text{ around } z \end{matrix}$$

*vector magnitude = 156.9 mm*

*Right:*

$$\begin{bmatrix} 0.9976 & 0.0125 & -0.0685 \\ -0.0111 & 0.9997 & 0.0212 \\ 0.0688 & -0.0203 & 0.9974 \end{bmatrix} \times \begin{bmatrix} -48.5 \\ 1.1 \\ 145.4 \end{bmatrix} = \begin{bmatrix} -58.4 \\ 4.7 \\ 141.7 \end{bmatrix} \equiv \begin{matrix} 1.5^\circ \text{ around } x \\ -3.9^\circ \text{ around } y \\ -3.3^\circ \text{ around } z \end{matrix}$$

*vector magnitude = 153.3 mm*

*Palate:*

Rotation of the jaw-joint around the dermopalatine-vomerine joint:

*Left:*

$$\begin{bmatrix} 0.9981 & 0.0023 & 0.0611 \\ -0.0038 & 0.9997 & 0.0240 \\ -0.0610 & -0.0242 & 0.9978 \end{bmatrix} \times \begin{bmatrix} 52.4 \\ 6.3 \\ 159.2 \end{bmatrix} = \begin{bmatrix} 62.1 \\ 9.9 \\ 155.5 \end{bmatrix} \equiv \begin{matrix} 1.4^\circ \text{ around } x \\ 3.5^\circ \text{ around } y \\ 2.2^\circ \text{ around } z \end{matrix}$$

*vector magnitude = 167.7 mm*

*Right:*

$$\begin{bmatrix} 0.9967 & -0.0097 & -0.0801 \\ 0.0099 & 1.0000 & 0.0019 \\ 0.0801 & -0.0027 & 0.9968 \end{bmatrix} \times \begin{bmatrix} -47.3 \\ 2.4 \\ 154.4 \end{bmatrix} = \begin{bmatrix} -59.5 \\ 2.2 \\ 150.1 \end{bmatrix} \equiv \begin{matrix} 0.0^\circ \text{ around } x \\ -4.6^\circ \text{ around } y \\ 0.7^\circ \text{ around } z \end{matrix}$$

*vector magnitude = 161.5 mm*

*Hyomandibula:*

Rotation of the distal-most ossified portion of the hyomandibula around the lateral commissure:

*Left:*

$$\begin{bmatrix} 0.9593 & -0.0504 & 0.2779 \\ 0.0207 & 0.9938 & 0.1089 \\ -0.2816 & -0.0987 & 0.9544 \end{bmatrix} \times \begin{bmatrix} 22.8 \\ 10.2 \\ 19.0 \end{bmatrix} = \begin{bmatrix} 26.6 \\ 12.7 \\ 10.7 \end{bmatrix} \equiv \begin{matrix} 21.5^\circ \text{ around } x \\ 17.9^\circ \text{ around } y \\ 1.3^\circ \text{ around } z \end{matrix}$$

*vector magnitude = 31.4 mm*

*Right:*

$$\begin{bmatrix} 0.9527 & -0.0648 & -0.2968 \\ 0.0901 & 0.9933 & 0.0722 \\ 0.2901 & -0.0955 & 0.9522 \end{bmatrix} \times \begin{bmatrix} -20.3 \\ 12.5 \\ 22.2 \end{bmatrix} = \begin{bmatrix} -26.7 \\ 12.2 \\ 14.0 \end{bmatrix} \equiv \begin{matrix} 11.6^\circ \text{ around } x \\ -19.8^\circ \text{ around } y \\ 7.1^\circ \text{ around } z \end{matrix}$$

*vector magnitude = 32.6 mm*

*Lower jaw:*

Rotation of the retroarticular process around the mandibular symphysis:

*Left:*

$$\begin{bmatrix} 0.9982 & -0.0131 & 0.0577 \\ 0.0122 & 0.9998 & 0.0168 \\ -0.0579 & -0.0160 & 0.9982 \end{bmatrix} \times \begin{bmatrix} 71.5 \\ 3.0 \\ 191.8 \end{bmatrix} = \begin{bmatrix} 82.4 \\ 7.1 \\ 187.3 \end{bmatrix} \equiv \begin{matrix} 1.3^\circ \text{ around } x \\ 3.3^\circ \text{ around } y \\ 2.5^\circ \text{ around } z \end{matrix}$$

*vector magnitude = 204.7 mm*

*Right:*

$$\begin{bmatrix} 0.9980 & -0.0089 & -0.0619 \\ 0.0091 & 1.0000 & 0.0028 \\ 0.0619 & -0.0034 & 0.9981 \end{bmatrix} \times \begin{bmatrix} -68.1 \\ 1.0 \\ 187.0 \end{bmatrix} = \begin{bmatrix} -79.5 \\ 0.9 \\ 182.4 \end{bmatrix} \equiv \begin{matrix} 0.0^\circ \text{ around } x \\ -3.6^\circ \text{ around } y \\ 0.2^\circ \text{ around } z \end{matrix}$$

*vector magnitude = 199.0 mm*



**Movie S1 (separate file) | Animation of cranial kinesis in *Tiktaalik roseae*.** Shown are the proposed rotations of cranial elements (in anterior, posterior, dorsal, and ventral views), from resting to expanded states, due to cranial kinesis. Color coding of anatomical units correspond to those shown in Figs. 2, 3, 4, S6, S7, S8: cheek (green), palate (yellow), skull roof (grey), braincase (cyan), vomers (purple), hyomandibula (red), and lower jaw (dark red). Rotation of the “palatoquadrate module” occurs at the dermopalatine-vomerine joint (dpt-vo, Figs. 2a, 3a, 4b), whereas rotation of the “hyomandibular module” occurs at the hyomandibular-lateral commissure (hy-lcm, Figs. 2a, 3a, 4b) (see text, 3D animation, Figs. S7, S8, Table S3).

**Movie S2 (separate file) | Animation of retrodeformation of the skull of *Tiktaalik roseae*.** Shown are the proposed transformations of cranial elements (in each of the cardinal views), from *in situ* to *in vivo* positions. Color coding of anatomical units correspond to those shown in Figs. 2, 3, 4, S6, S7, S8: cheek (green), palate (yellow), skull roof (grey), braincase (cyan), vomers (purple), hyomandibula (red), and lower jaw (dark red). Reconstruction of life-like positions involved rotation and translation of cranial elements only without the use of scaling or plastic deformation (see text, limited retrodeformation, Figs. S6, S7, Table S2).